Colloids and Surfaces B: Biointerfaces 110 (2013) 254–260

Contents lists available at SciVerse ScienceDirect

Colloids and Surfaces B: Biointerfaces

journal homepage: www.elsevier.com/locate/colsurfb

Transdermal delivery of betahistine hydrochloride using microemulsions: Physical characterization, biophysical assessment, confocal imaging and permeation studies

Rania M. Hathout*, Maha Nasr

Department of Pharmaceutics and Industrial Pharmacy, Faculty of Pharmacy, Ain Shams University, Cairo, Egypt

ARTICLE INFO

Article history:
Received 22 February 2013
Received in revised form 3 May 2013
Accepted 7 May 2013
Available online 13 May 2013

Keywords:
Microemulsion
Skin resistance
Pseudoplastic
Transdermal
Confocal

ABSTRACT

Transdermal delivery of betahistine hydrochloride encapsulated in various ethyl oleate, Capryol 90®, Transcutol® and water microemulsion formulations was studied. Two different kinds of phase diagrams were constructed for the investigated microemulsion system. Pseudoplastic flow that is preferable for skin delivery was recorded for the investigated microemulsions. A balanced and bicontinuous microemulsion formulation was suggested and showed the highest permeation flux ($0.50 \pm 0.030\ mg\ cm^{-2}\ h^{-1}$). The effect of the investigated microemulsions on the skin electrical resistance was used to explain the high permeation fluxes obtained. Confocal laser scanning microscopy was used to confirm the permeation enhancement and to reveal the penetration pathways. The results obtained suggest that the proposed microemulsion system highlighted in the current work can serve as a promising alternative delivery means for betahistine hydrochloride.

1. Introduction

Betahistine hydrochloride [*N*-methyl-2-(pyridin-2-yl) ethanamine dihydrochloride], which acts as an active histamine analogue, is a very interesting drug that aroused the curiosity of scientists since it was first synthesized [1,2]. Early attempts for its use centred on the ability of this compound to cause vasodilatation in the cerebral vasculature region, and hence, it has been used to reduce and relieve the symptoms of vertigo, tinnitus, and hearing loss associated with Ménière's disease [3]. With the expanding knowledge on histamine, in general, and on its role as a neurotransmitter in particular, potential new interesting indications for this compound have emerged especially in the regulation of feeding behaviour and weight control [4].

Betahistine is usually given by the oral route as the hydrochloride salt. The short half life of this drug (3–4 h) necessitates its frequent dosing [3]. Usually, the initial dose ranges from 8 to 16 mg taken three times daily preferably with meals. Maintenance doses are generally in the range 24–48 mg daily. Unfortunately, betahistine has histamine like action on the secretory cells of the gastric mucosa and hence its use is un-preferred in patients with gastric irritation or peptic ulcer [5,6]. In a clinical study conducted on eleven patients diagnosed with a definite Ménière's disease where oral betahistine hydrochloride was administered, various related side effects including gastrointestinal complaints, fatigue and after taste in 46% of the patients were reported [7]. The aforementioned facts warrant the search for a new route of administration viz. the transdermal route. Moreover, the high aqueous solubility of the drug requires specific technologies in order to control its release and delivery maintaining the concentration of the drug within the therapeutic range and eliminating the intolerance drawback that is usually associated with the immediate release conventional oral dosage forms [5,8]. Development of transdermal formulations for betahistine hydrochloride is challenging again because of its high solubility which makes its penetration through the stratum corneum (SC) (epidermis outermost and highly lipophilic layer) a difficult task. To this end, topical microemulsions could be considered an ideal solution.

Microemulsions are monophasic, optically isotropic and thermodynamically stable systems with a droplet size typically in the range 10–100 nm. They are considered more stable than topical vesicular systems like liposomes, ethosomes, niosomes, etc. They are translucent mixtures of oil, surfactant, cosurfactant, and water, in which either the oil globules are dispersed in water (o/w) or water globules are dispersed in oils (w/o) or else domains of oil and water co-exist together (bicontinuous) [9]. The use of microemulsions in skin drug delivery has been frequently exploited and has proven highly successful for the delivery of hydrophilic and lipophilic compounds [10–12].

* Corresponding author. Tel.: +20 1 005254919/2 22912685; fax: +20 2 0224011507.
E-mail addresses: r_hathout@yahoo.com, rania.hathout@pharma.asu.edu.eg (R.M. Hathout).

0927-7765/$ – see front matter © 2013 Elsevier B.V. All rights reserved.
http://dx.doi.org/10.1016/j.colsurfb.2013.05.007

Many mechanisms were reported for the transdermal delivery from microemulsions; first, microemulsions allow for high drug loading capacities, second, the microemulsion components exhibit a powerful penetration enhancing effect [13,14], third, the microemulsion components can possibly enter into the skin as monomers [15,16], increasing the solubility of the drug in the skin, fourth, the microstructure of the system provides large surface area for drug transfer and diffusion and finally, the phase transition of microemulsions provides a possibility for producing a supersaturated system with a high thermodynamic activity [17].

The present study was attempted to investigate the potential development of novel nano-colloidal formulations for the successful delivery of betahistine hydrochloride through an alternative route; the transdermal route. In this perspective, a microemulsion system was developed and physically characterized. Microemulsion formulations were selected and were subjected to ex-vivo permeation testing and laser confocal microscopic imaging. Physical and biophysical assessments were also attempted to evaluate the performance of the investigated microemulsion formulations and to record their effects on the skin barrier.

2. Materials and methods

2.1. Skin

Full male albino mouse skin was used in all the experiments. The animal was obtained from a local farm. The skin was cleaned carefully under cold running water and was stored frozen at −20°C for a period no more than one month before use.

2.2. Materials

Betahistine hydrochloride was kindly provided by the Egyptian International Pharmaceutical Industries Co. EIPICO (EIPICO, ELSharqia, Egypt). Bisdemethoxycurcumin, ethyl oleate, orthophosphoric acid, sodium lauryl sulphate and triethylamine were purchased from Sigma–Aldrich (Sigma–Aldrich, Gillingham, UK). Diethylene glycol monoethyl ether (Transcutol®) and propylene glycol monocaprylate (Capryol 90®) were kindly provided by Gattefosse' (Gattefosse', Lyon, France). Acetonitrile, (HPLC grade) (Fisher Scientific, Loughbrough, UK), sodium chloride, potassium chloride, sodium phosphate (monobasic) and potassium phosphate (dibasic) were purchased from Acros Organics (Acros Organics, Geel, Belgium). Parafilm® was purchased from Pechiney Co. (Pechiney plastic packaging company, Chicago, IL, USA). All aqueous solutions were prepared using high-purity deionized water with conductance less than 1 $\mu S\,cm^{-1}$ (18.2 MΩ cm) (Barnstead Nanopure Diamond, Dubuque, IA, USA).

2.3. Methods

2.3.1. Phase diagrams

2.3.1.1. Kahlweit phase diagram. Kahlweit fish presentation, where the phase domains were determined with respect to two variables; concentration of surfactants and temperature, was used to construct a phase diagram [18]. This diagram helps in confirming the microemulsion forming ability of the chosen components at the skin temperature (32 °C) and at an equal proportion of oil and water.

Ethyl oleate® was chosen as the oily phase. The surfactant system included Capryol 90® as the surfactant and Transcutol® as the co-surfactant. Water comprised the aqueous phase.

The percentage of the surfactant mixture was varied for a fixed oil/water ratio = 1/1. The different microemulsions were prepared by mixing the different components (oil, water and surfactant mixture) under magnetic stirring. Preparations were placed in ovens at different temperatures (from 10 °C to 70 °C with 10 °C steps) for equilibration. Samples were designated as monophasic (clear) (1Φ), diphasic (2Φ) with an oil excess phase (o/w microemulsion + oil) or with a water excess phase (w/o microemulsion + water), or triphasic (3Φ) (bicontinuous microemulsion + oil + water). Samples were observed under polarized microscope (Olympus BX51 U-AN 360, Tokyo, Japan) between crossed polars to confirm the isotropic nature of the obtained microemulsions [19].

2.3.1.2. Pseudoternary phase diagram at constant temperature. The phase diagram was constructed using the water dilution titration method at ambient temperature (25 °C) as previously described elsewhere [20,21]. The Pseudo-ternary phase diagram was prepared with the weight ratio of 1:1 Capryol 90® to Transcutol®.

Selected microemulsion formulations were chosen from the microemulsion obtained domain.

2.3.2. Preparation of betahistine microemulsions

For all the selected formulae, first, betahisitine (3%, w/v) was dissolved gradually in the aqueous phase. Second, Ethyl oleate, Capryol 90® and Transcutol® were mixed under magnetic stirring. Third, the aqueous phase was added gradually to the oil/surfactants mixture. Magnetic stirring was used to aid rapid emulsification.

2.3.3. Particle size measurements

The particle size and the polydispersity index of the chosen microemulsions were determined using dynamic light scattering (Malvern Zetasizer, Malvern, Worcestershire, UK). The viscosity was adjusted at 0.05 Pa S. The scattering intensity data were obtained after pre-filtering (0.45 μm) the microemulsions. The samples were loaded into cuvettes 1 ml in volume and the temperature was set at 25 °C. Triplicate measurements were performed.

2.3.4. Rheological measurements

The viscosity of the prepared microemulsions was measured with a DV-E Viscometer (Brookfield Engineering Laboratories, Middleboro, MA, USA) using a 61 spindle [22,23] at speeds ranging from 0.5 to 100 rpm, at room temperature, and over 10% torque.

2.3.5. Ex-vivo permeation and data analysis

2.3.5.1. Ex-vivo permeation. Male albino mouse skin was defrosted, cut into square pieces that were mounted with the stratum corneum uppermost in Franz-type diffusion cells (Permegear, Hellertown, PA, USA). The receptor volume was 7.5 ml and the diffusional area was 1.77 cm^2. Before starting the permeation experiment, the receptor solution was filled with phosphate buffered saline (PBS) at pH 7.4 and magnetically stirred. The skin surface was covered with 1 ml of the same solution at 37 °C for 1 h. Subsequently, the PBS in the donor was replaced by 1 ml of the prepared microemulsions containing 3% (w/v) betahistine and the compartment was covered with Parafilm®. One millilitre sample was collected to be analyzed at 0.5, 1, 2, 3, 4, 6, 8 and 24 h and immediately replaced with fresh buffer. All the samples were filtered using 0.45 μm Nalgene® Millipore syringe filters (Thermo Fisher Scientific, Waltham, MA, USA) prior to analysis. All the permeation experiments were performed in triplicates. Betahistine in the samples was quantified using high performance liquid chromatography.

2.3.5.2. Detection of betahistine using high performance liquid chromatography. Quantification of betahistine was achieved using an HPLC system (Agilent, Santa Clara, CA) consisting of a pump, a UV detector, and a C18 column (Agilent Eclipse column XDB-C18 (5 μm, 4.6 × 150 mm)). The mobile phase consisted of a 60% aqueous solution: 40% acetonitrile. The aqueous solution consisted of 0.67% (v/v) triethylamine and 0.33% (w/v) sodium lauryl sulphate

adjusted to pH 3.5 using orthophosphoric acid. The flow rate of the mobile phase was 0.3 ml/min at 30 °C. The injection volume was 10 μl and the column effluent was monitored at 254 nm.

2.3.5.3. Data analysis. The permeation results from each prepared microemulsion formulation were expressed as the cumulative amount of drug permeated across the skin barrier per unit area (Q) as a function of time (t). Each permeation curve was fitted to the appropriate solution (Eq. (1)) of the non-steady state diffusion equation (Fick's second law [24]), which assumes the following boundary conditions: (a) that there is no depletion of the drug in the donor compartment over the whole period of the experiment, (b) that the receptor phase provides "sink condition" for the drug, and (c) that at $t = 0$, there is no drug in the skin [25]. That is,

$$Q = \{KH\}C_{veh}\left[\left(\frac{D}{H^2}t - \frac{1}{6} - \frac{2}{\pi^2}\sum_{n=1}^{\infty}\frac{(-1)^n}{n}\exp\left(\frac{-Dn^2\pi^2 t}{H^2}\right)\right)\right] \quad (1)$$

where C_{veh} is the drug's concentration in the donor solution; K is its SC-microemulsion partition coefficient and D is the diffusivity of the drug in the SC of thickness H. The fitting procedure was performed using a commercial software package (Prism, Version 5, GraphPad Software, San Diego, CA, USA), running on a personal computer. Accordingly, the drug's characteristic diffusivity (D/H^2) and partitioning (KH) parameters were obtained. Permeability coefficients were calculated as the product of these two parameters and consequently the permeation fluxes were calculated as follows:

$$J_{ss} = k_p \times C_{veh} \quad (2)$$

where J_{ss} is the obtained steady state flux of the drug; k_p is the permeability coefficient and C_{veh} is the concentration of the drug in the microemulsion formulation.

2.3.6. Microemulsions effect on the electrical resistance of the skin

To evaluate the effect of the microemulsions on the barrier function of the skin, the electrical resistance of the tissue was measured before and after application of aqueous buffer pH 7.4 (control), ME1, ME2 and ME3 using an LCR multimeter (Mod. 179, accuracy 0.8%, Fluke, Everett, WA). Skin samples were mounted in diffusion cells, and the donor and receptor compartments were filled with PB 7.4; after 20 min of equilibration (allowing the SC to come to a steady state [26], the electrodes were inserted in the donor and receptor compartments for measurement of baseline skin resistance. After, the phosphate buffer in the donor compartment was replaced with 1 ml of the control or the investigated microemulsions for 24 h. By the end of the experiment, skin samples were rinsed with water and carefully blotted dry. The donor compartment was then refilled with PB 7.4, and the electrical resistance was hence recorded [11,27]. Fig. 1 demonstrates the aforementioned experiment setup.

2.3.7. Confocal microscopy studies

For confocal laser scanning microscopy, a fluorescent dye; bisdemethoxycurcumin (0.1%, w/v) was incorporated in the selected microemulsion formulation (ME2). The fluorescent microemulsion was applied to the skin for 24 h, after which the skin was removed from the diffusion cell, rinsed with 50% ethanol and then the surface of the skin was wiped gently. The skin was directly sandwiched between a glass slide and a cover slip and examined using invert laser scanning confocal microscope (LSM 710, Carl Zeiss, Jena, Germany) without additional tissue processing [28]. The fluorescence of bisdemethoxycurcumin was excited at a wavelength of 488 nm by means of an argon laser [29], which is reported to excite curcumin and its derivatives efficiently [28]. The fluorescence signal was detected at 590 nm. Curcumin and curcuminoids emission

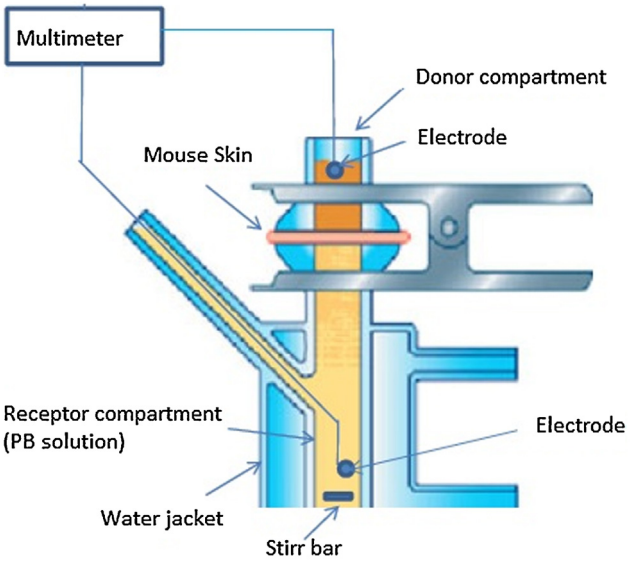

Fig. 1. Experiment setup for skin electrical resistance measurement.

signals were successfully detected at this wavelength which is far from the background fluorescence caused by the skin protein bands [30]. The skin sample was scanned from the skin surface (0 μm) to a depth of 20 μm m at a 1 μm interval. The skin was then inspected under a 63x objective lens (EC-Plan Neofluar 63x/01.40 Oil DIC M27). Images were obtained in the *xy* and *xz* planes (optical sectioning z-stack mode). Confocal images were recorded and further processed using LSM Image Browser software, release 4.2 (Carl Zeiss microimaging, Gottingen, GMBH) [16].

3. Results and discussion

3.1. Phase diagrams

3.1.1. Kahlweit phase diagram

Fig. 2 represents the Kahlweit phase diagram demonstrating the number of phases obtained after varying the surfactant/cosurfactant mixture percentage and temperature. The figure shows a monophasic region obtained at surfactant percentages above 60% (w/w) and at wide range of temperatures including

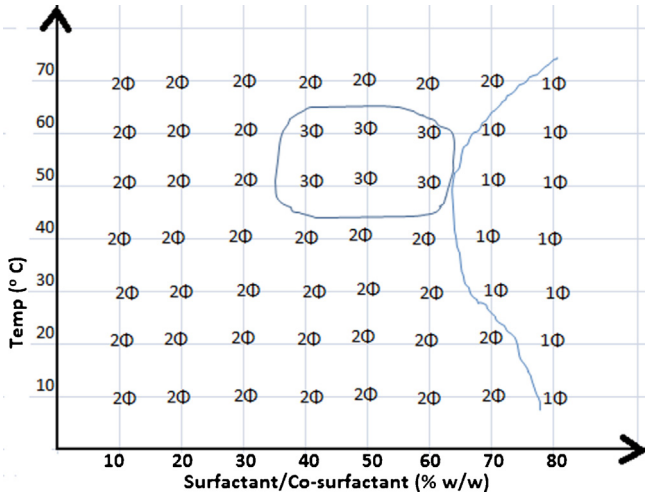

Fig. 2. Kahlweit phase diagram for the microemulsion system ethyl oleate, Capryol 90®, Transcutol® and water.

The Selected Microemulsion Formulations (%w/w)

	ME 1	ME 2	ME 3
Ethyl Oleate	40	15	10
Capryol 90®	27.5	35	35
Transcutol®	27.5	35	35
Water	5	15	20

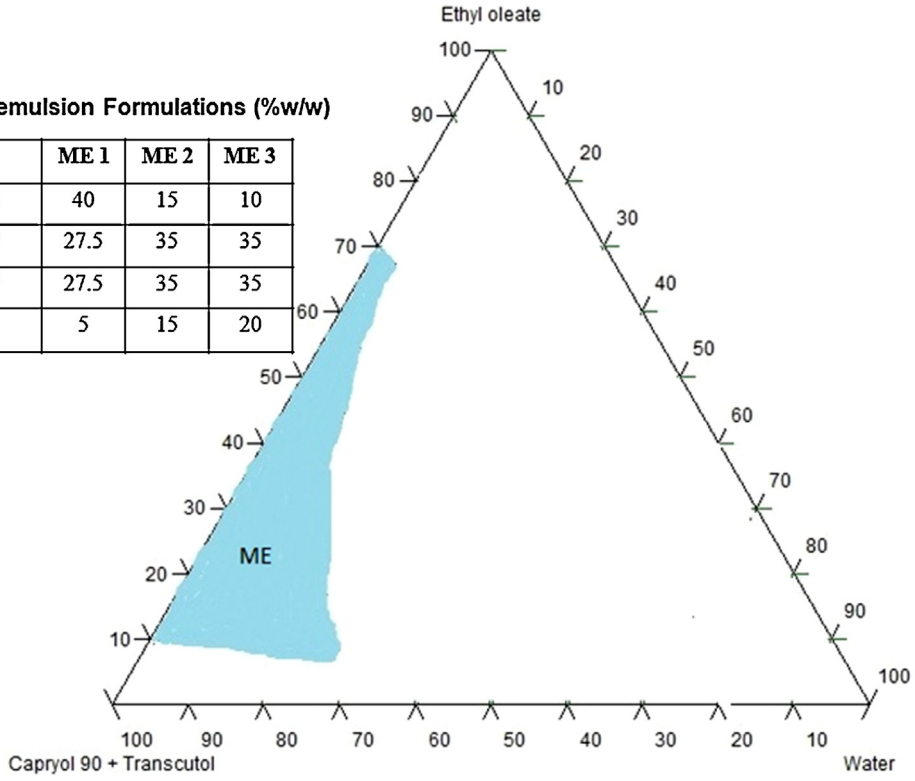

Fig. 3. Pseudoternary phase diagram of the microemulsion system ethyl oleate, Capryol 90®, Transcutol® and water, at constant temperature. The table shows the composition of the studied microemulsion formulations.

room temperature and 32 °C (the normal temperature of human and animals skin) [18,19].

3.1.2. Pseudoternary phase diagram at constant temperature

Fig. 3 shows the microemulsion domain area in the pseudoternary phase diagram constructed using ethyl oleate as the oily phase, Capryol 90® as the surfactant, Transcutol® as the cosurfactant and water as the aqueous phase. Transcutol as a small and balanced surface active molecule can intercalate the Capryol 90 (surfactant) film at the interface between the oil and water, decreasing the interfacial tension to very low values allowing for the formation of microemulsions [9].

Three different formulae were selected across this domain (as demonstrated in the table in Fig. 3) with varying compositions of water and oil where the drug betahistine hydrochloride was incorporated and the microemulsions were physically characterized.

3.2. Particle size measurement

The *z*-average diameter recorded for ME1 and ME3 was 16.34 ± 5.58 and 8.2 ± 1.34 with polydispersity indices of 0.382 ± 0.05 and 0.137 ± 0.05, respectively. This small particle size together with its narrow distribution indicates the presence of droplet microemulsions and explains the clarity and isotropicity of the formulations. Particle size measurements could not be obtained for ME2. Large fluctuations in particle size measurement were observed and high polydipersity indices (>0.84) were recorded. These findings assume a bicontinuous structure for ME2. The dynamic nature of this type accompanied with high surfactant exchange processes occurring at the oil/water interface hinders the particle size measurement [31].

3.3. Rheological measurements

Fig. 4 shows the rheograms obtained for the three investigated microemulsions where it demonstrates the pseudoplastic and shear-thinning behaviour of all of them. Several previous studies confirmed this rheological pattern for microemulsions [32,33]. The shear-thinning behaviour is usually preferred so that the applied skin systems would be stable at rest, nevertheless upon application on the skin the viscosity decreases and drug permeation is enhanced.

3.4. Ex vivo permeation results

Betahisitne hydrochloride has an expected poor skin permeability according to the mathematical model derived by Potts and Guy where the increase in drug permeability coefficient is

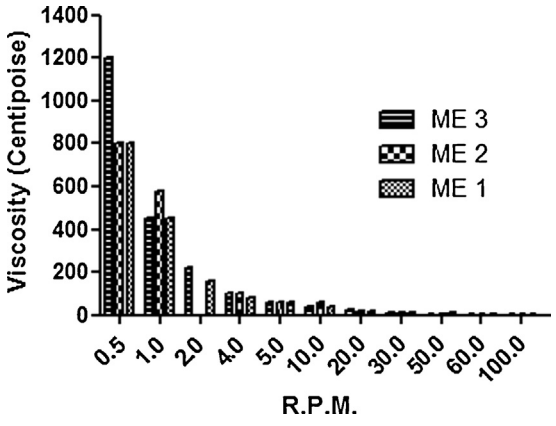

Fig. 4. Viscosity measurements of the investigated microemulsion formulations.

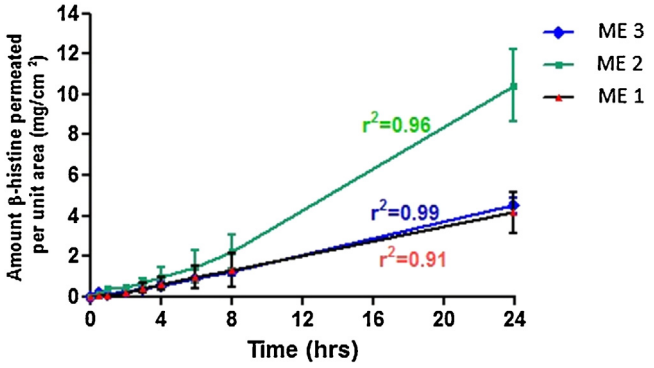

Fig. 5. Ex vivo permeation of Betahistine hydrochloride from the investigated microemulsion formulations.

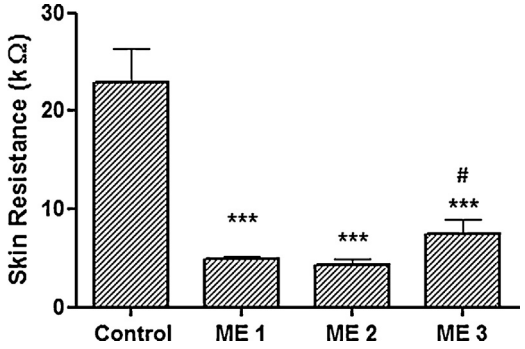

Fig. 6. Effect of treatment of buffer and the investigated microemulsion formulations on the skin electrical resistance. Each point represents means ± standard deviation of 4 replicates $^{***}p < 0.001$ compared to buffer and $^{\#}p < 0.05$ compared to ME2.

directly related to its lipophilicity [34]. Accordingly, the prepared microemulsion formulations comprising oil and surfactants as penetration enhancers were chosen to solve this permeability problem. Fig. 5 demonstrates the permeation profiles of betahistine hydrochloride from the three investigated microemulsions. All three profiles show excellent fitting with Fick's second law of diffusion ($r^2 > 0.90$ for all the formulae). ME2 showed the highest permeation flux ($0.50 \pm 0.030\ mg\ cm^{-2}\ h^{-1}$) and the cumulative amount permeated after 24 h reached $10.42 \pm 1.8\ mg\ cm^{-2}$. One way ANOVA between the results of the amount of betahistine hydrochloride permeated after 24 h for the three microemulsion formulations followed by Tukey Karmer's test to compare between all the pairs, showed the significant difference between ME2 (Balanced and bicontinuous microemulsion) and the other prepared microemulsions at $p < 0.05$. It has been previously reported in the literature that higher transdermal permeation potential could be obtained using balanced water and oil microemulsion formulations [12,20,35,36]. Table 1 compares the three microemulsion formulations regarding the partitioning, the diffusivity and the fluxes obtained. Moreover, the bicontinuous structure of microemulsions with alternating aqueous and oily domains was proven to be highly compatible with the skin structure. Additionally, these highly dynamic and fluctuating surfactant-film structures lead to relatively faster diffusion and release of drugs resulting in higher skin fluxes [6] compared to the results previously obtained in a study adopted on betahistine hydrochloride delivered transdarmally from an adhesive transdermal patch [37]. More than ten-fold increase in skin fluxes and permeability coefficients were recorded. The highest diffusivity result scored for ME2 (Table 1) confirms these suggestions. Diffusivity through the skin was directly correlated with the self-diffusion of a model drug in its vehicle in a recent work by Hathout and Woodman [38]. The high fluxes obtained are attributed to the different penetration enhancers present in the microemulsion formulations such as: ethyl oleate (possessing a lipophilic nature which increases the fluidity of the stratum corneum of the skin [39] in addition to its unsaturated structure which was previously proven to enhance the transdermal delivery of different compounds) and Transcutol® which was previously proven to partition into the SC [14]. Additionally, the water present in the microemulsions contributes to skin hydration which plays a very important role in enhancing drug delivery through the skin [40].

Table 1
Drug partitioning (KH) and diffusivity (D/H^2) parameters, permeability coefficients (k_p) and steady-state Fluxes (J_{ss}) of Betahistine (3%, w/v) from different microemulsions containing ethyl oleate/Capryol 90®/Transcutol®/water across mouse skin ex vivo.

ME	KH (cm)	D/H^2 (h^{-1})	$10^2 \times k_p$ (cm/h)	J_{ss} ($mg\ cm^{-2}\ h^{-1}$)
1	0.023 ± 0.02	0.26 ± 0.03	0.6 ± 0.5	0.18 ± 0.014
2	0.028 ± 0.08	0.59 ± 0.01	1.7 ± 0.01	0.50 ± 0.030
3	0.033 ± 0.01	0.18 ± 0.06	0.6 ± 0.06	0.18 ± 0.020

3.5. Effect of the investigated microemulsions on the electrical resistance of the skin

Compared to the control, all the studied microemulsions significantly ($p < 0.001$) decreased the skin resistance after application for 24 h (Fig. 6). The effect of ME2 was more intense. These results confirm the superiority of the microemulsions in disrupting and reversibly decreasing the skin barrier function and consequently its electrical resistance [11]. It is worth noting that there was no significant difference between ME1 and ME2 in decreasing the skin resistance. While ME1 possess high surfactants and oil contents that contribute in decreasing the skin resistance, ME2 bicontinuous dynamic and fluctuating structures have distinguished penetrating ability and disrupting effects on the skin architecture and hence its barrier properties viz. electrical resistance. These results give more insight on and suggest another explanation for the high penetration fluxes obtained for ME2.

3.6. Confocal microscopy results and significance

The confocal laser scanning microscopy (CLSM) imaging provides information about the extent and pathways of skin permeation. The principal advantages of this technique are good time-resolution, potential in vivo applicability, and multi-depth imaging parallel to the skin surface without a need for mechanical sectioning or tissue processing [41].

Fig. 7(a) demonstrates the permeation of the studied microemulsion across the skin main barrier (i.e. the SC). High fluorescence intensities were maintained across the SC whole depth (20 μm) indicating the high potential of the investigated bicontinuous microemulsion for transdermal delivery (Fig. 7(b)). CLSM image at the skin surface (Fig. 7(c)) revealed that the paracellular, intercellular and appendageal routes provided different paths for skin permeation for the investigated microemulsion. This finding was concluded from the high fluorescence observed inside a corneocyte (yellow circled), at the corneocyte border delineating its hexagonal structure indicating the permeation of the microemulsion through the intercellular lipids and near hair follicles (white circled).

The imaged hair follicles were spotted at $x = 254$ and $y = 536$ in the 712×712 xy image (yellow circled in Fig. 7(d)). The high fluorescence observed in this position (around the investigated hair follicles) indicates the accumulation of the microemulsion at this area which confirms this appendage as a permeation route. Lipid

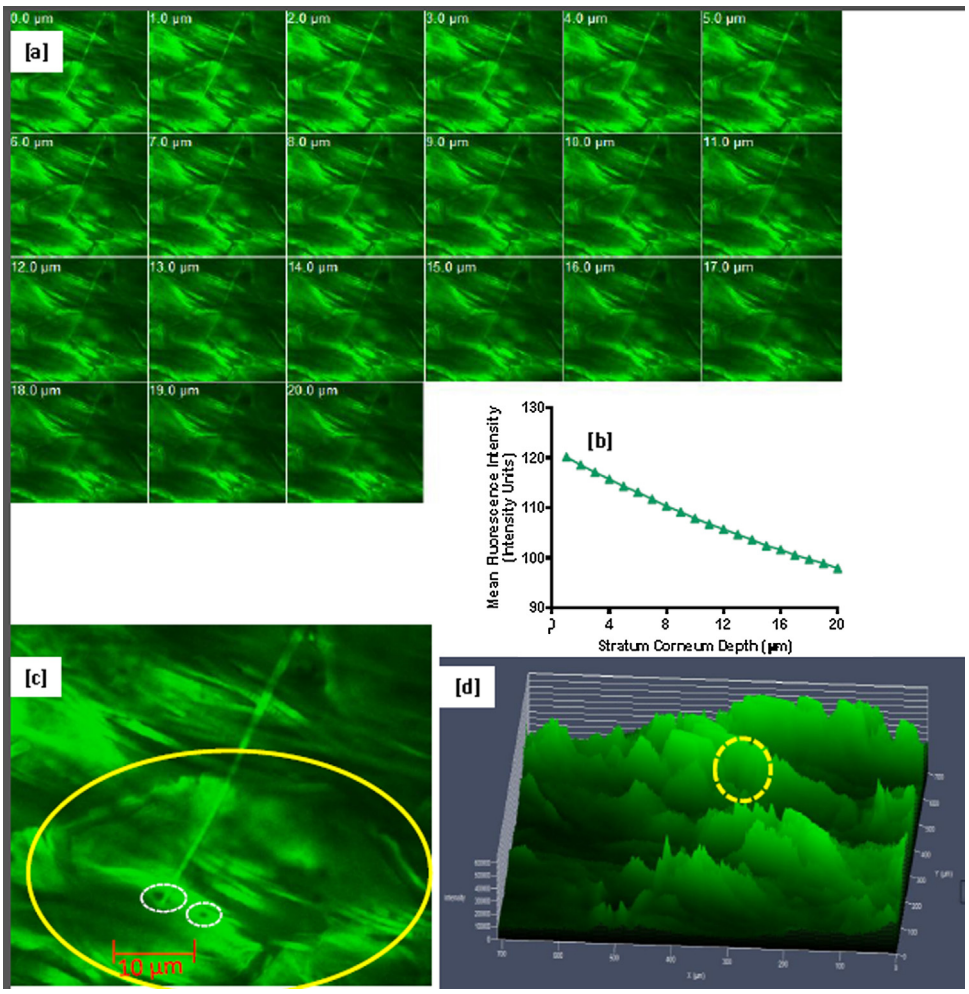

Fig. 7. (a) z-stack image of ME2 fluorolabelled with bisdemethoxy curcumin (the stratum corneum was sectioned from 0 to 20 µm with 1 µm increments). (b) Mean fluorescence intensities of bisdemethoxy curcumin across the stratum corneum depth. (c) A 1024 × 1024 surface *xy* image of the stratum corneum (a corneocyte is yellow circled and hair follicles openings are white circled). (d) A 712 × 712 3D plot of the same *xy* image in (c) showing the dye fluorescence intensities (the place of hair follicles is localized and yellow centred). (For interpretation of the references to colour in this figure legend, the reader is referred to the web version of the article.)

disperse systems were previously clarified to be incorporated in the intercellular domains of the stratum corneum and follicles. Moreover, the fluidity of the SC lipid was found to significantly increase as a result of incorporation of fluid lipids, e.g. ethyl oleate and Capryol 90®, thus ensuring the rapid permeation of the fluid lipid disperse system e.g. microemulsion into the SC and the viable epidermis [42,43].

4. Conclusion

Transdermal delivery, as a novel alternative route, of betahistine hydrochloride was accomplished successfully using a balanced bicontinuous microemulsion formulation comprising ethyl oleate, Capryol 90®, Transcutol® and water. Different mechanisms of permeation enhancement as well as various penetration pathways were postulated.

Acknowledgements

R.M. Hathout is sincerely grateful to professor R.H. Guy, Department of Pharmacy and Pharmacology at the University of Bath in the UK, for his help, support, useful and instructive discussions. The authors would also like to acknowledge the Egyptian International Pharmaceutical Industries Co. EIPICO for their kind supply of betahistine hydrochloride and Gattefosse' company, France for their kind supply of Capryol 90® and Transcutol®.

References

[1] N. Barak, Exp. Opin. Investig. Drugs 17 (2008) 795.
[2] A. Khedr, M. Sheha, J. Chromatogr. B Analyt. Technol. Biomed. Life Sci. 869 (2008) 111.
[3] S.C. Sweetmant, MartinDale, The Complete Drug Reference, Pharmaceutical Press, London, 2009.
[4] A. Szelag, M. Trocha, A. Merwid-Lad, Pol. J. Pharmacol. 53 (2001) 701.
[5] R.N. Shamma, E.B. Basalious, R.A. Shoukri, Int. J. Pharm. 405 (2011) 102.
[6] A.A. Heda, A.R. Sonawane, G.H. Naranje, V.G. Somani, P.K. Pauranik, Trop. J. Pharm. Res. 9 (2010) 516.
[7] F. Lezius, C. Adrion, U. Mansmann, K. Jahn, M. Strupp, Eur. Arch. Otorhinolaryngol. 268 (2011) 1237.
[8] R.N. Shamma, E.B. Basalious, R. Shoukri, Pharm. Dev. Technol. 17 (2012) 583.
[9] M.J. Lawrence, G.D. Rees, Adv. Drug Deliv. Rev. 45 (2000) 89.
[10] R.M. Al Abood, S. Talegaonkar, M. Tariq, F.J. Ahmad, Colloids Surf. B Biointerfaces 101 C (2012) 143.
[11] L.B. Lopes, H. VanDeWall, H.T. Li, V. Venugopal, H.K. Li, S. Naydin, J. Hosmer, M. Levendusky, H. Zheng, M.V. Bentley, R. Levin, M.A. Hass, J. Pharm. Sci. 99 (2010) 1346.
[12] J. Zhang, B. Michniak-Kohn, Int. J. Pharm. 421 (2011) 34.
[13] R.M. Hathout, A.H. Elshafeey, Eur. J. Pharm. Biopharm. 82 (2012) 230.
[14] R.M. Hathout, T.J. Woodman, S. Mansour, N.D. Mortada, A.S. Geneidi, R.H. Guy, Eur. J. Pharm. Sci. 40 (2010) 188.
[15] R.M. Hathout, S. Mansour, A.S. Geneidi, N.D. Mortada, J. Colloid Interface Sci. 354 (2011) 124.
[16] R.M. Hathout, S. Mansour, N.D. Mortada, A.S. Geneidi, R.H. Guy, Mol. Pharmacol. 7 (2010) 1266.

[17] G. El Maghraby, Curr. Nanosci. 8 (2012) 504.
[18] M. Kahlweit, Microemulsions, Science 240 (1988) 617–621.
[19] W. Naoui, M.A. Bolzinger, B. Fenet, J. Pelletier, J.P. Valour, R. Kalfat, Y. Chevalier, Pharm. Res. 28 (2011) 1683.
[20] H. Chen, X. Chang, T. Weng, X. Zhao, Z. Gao, Y. Yang, H. Xu, X. Yang, J. Control. Release 98 (2004) 427.
[21] N. Garti, V. Clement, M. Fanun, M.E. Leser, J. Agric. Food Chem. 48 (2000) 3945.
[22] H.J. Cho, W.S. Ku, U. Termsarasab, I. Yoon, C.W. Chung, H.T. Moon, D.D. Kim, Int. J. Pharm. 423 (2012) 153.
[23] Y.T. Zhang, Z.B. Huang, S.J. Zhang, J.H. Zhao, Z. Wang, Y. Liu, N.P. Feng, Int. J. Nanomedicine 7 (2012) 2465.
[24] D.R. Friend, J. Control. Release 18 (1992) 235.
[25] N. Sekkat, Y.N. Kalia, R.H. Guy, Pharm. Res. 21 (2004) 1390.
[26] G. Lu, D.J. Moore, Int. J. Cosmet. Sci. 34 (2012) 74.
[27] D. Pepe, J. Phelps, K. Lewis, J. DuJack, K. Scarlett, S. Jahan, E. Bonnier, T. Milic-Pasetto, M.A. Hass, L.B. Lopes, Int. J. Pharm. 434 (2012) 420.
[28] C.H. Liu, F.Y. Chang, Chem. Pharm. Bull. 59 (2011) 172.
[29] B. Champekam, V.A. Parthasarathy, Turmeric, in: V.A. Parthasarathy, B. Champekam, T.J. zachariah (Eds.), Chemistry of Spices, CABI, Oxford, 2008, p. 97.
[30] N. Otberg, H. Richter, H. Schaefer, U. Blume-Peytavi, W. Sterry, J. Lademann, Visualization of topically applied fluorescent dyes in hair follicles by laser scanning microscopy, Laser Phys. 13 (2003) 761–764.
[31] M. Fanun, J. Dispers. Sci. Technol. 33 (2012) 185.
[32] A. Kogan, D.E. Shalev, J. Phys. Chem. B 113 (2009) 10669.
[33] M.A. Moreno, M.P. Ballesteros, P. Frutos, J. Pharm. Sci. 92 (2003) 1428.
[34] R.O. Potts, R.H. Guy, Pharm. Res. 9 (1992) 663.
[35] H.Z. Liu, Y.J. Wang, Y.Y. Lang, H.M. Yao, Y. Dong, S.M. Li, J. Pharm. Sci. 98 (2009) 1167.
[36] Y.S. Rhee, J.G. Choi, E.S. Park, S.C. Chi, Int. J. Pharm. 228 (2001) 161.
[37] H.Z. Liu, S.M. Li, Y.J. Wang, F. Han, Y. Dong, Drug Dev. Ind. Pharm. 32 (2006) 549.
[38] R.M. Hathout, T.J. Woodman, J. Control. Release 161 (2012) 62.
[39] G.M. El Maghraby, F.K. Alanazi, I.A. Alsarra, Drug Dev. Ind. Pharm. 35 (2009) 329.
[40] P. Karande, S. Mitragotri, Biochim. Biophys. Acta 1788 (2009) 2362.
[41] V.M. Meidan, Exp. Opin. Drug Deliv. 7 (2010) 1095.
[42] T. Ogiso, N. Niinaka, M. Iwaki, J. Pharm. Sci. 85 (1996) 57.
[43] T. Ogiso, N. Niinaka, M. Iwaki, T. Tanino, Int. J. Pharm. 152 (1997) 135.